Primary Synchronization Signal Design for New Radio Technique in 5G Communication System

Yuexia He, Yi Gu, Shuqing Bu, Zhendong Mao
Key Laboratory of Universal Wireless Communications, Beijing University of Posts & Telecommunications
Beijing, China 100876
zhaozhongyuan_bupt@163.com

ABSTRACT

System synchronization between the user equipment (UE) and the base station (eNodeB) is a fundamental physical layer procedure in the cellular system and performed by synchronization signal. New Radio (NR) synchronization signal is expected to have the wider band reserved, which enables the use of the longer sequence than that in Long Term Evolution (LTE). This paper simulates the downlink (DL) initial synchronization procedure for NR in 5G and evaluates the NR primary synchronization signal (NR-PSS) design with various lengths. To accomplish the DL initial synchronization at the UE, the NR-PSS is firstly detected in the time domain using a matched filter, and then the carrier frequency offset (CFO) is the sum of the integer frequency offset (IFO) and the sum of the fractional frequency offset (FFO). After compensating the CFO of the received signal, we detect the NR second synchronization signal (NR-SSS) in the frequency domain. To evaluate the NR-PSS design with various lengths, the performance of the residual timing offset and residual frequency offset is considered. The simulation results show that the performance of the residual timing offset with the longer sequences is better and the length of the NR-PSS has no impact on the performance of the residual frequency offset. Thus we propose longer sequences in the NR-PSS design when the performance of the residual timing offset and the residual frequency offset is only considered.

KEYWORDS

5G, 5G New Radio, DL initial synchronization, simulation, NR-PSS design

ACM Reference format:
Yuexia He, Yi Gu, Shuqing Bu, Zhendong Mao. 2017. Primary Synchronization Signal Design for New Radio Technique in 5G Communication System. In *Proceedings of ACM Mobimedia conference, Chongqing, China, July 2017 (MOBIMEDIA'17),* 5 pages.
DOI: 10.1145/nnnnnnn.nnnnnnn

MOBIMEDIA'17, Chongqing, China

DOI: 10.1145/nnnnnnn.nnnnnnn

1 INTRODUCTION

In the next few years, with an explosively increasing data traffic in mobile broadband communications, the existing cellular networks might not be able to satisfy the users' demands [1]. Consequently, the fifth generation (5G) wireless cellular network has been intensively researched both in industries [2][3] and in academia [4]-[6] in recent years. To enable the expected 5G network, a new air interface (AI) is designed to effectively improve spectral efficiency and reduce latency [3]. One of the fundamental AI physical layer procedures is the system synchronization between the UE and the eNodeB.

In a cellular system, system synchronization is firstly finished in DL and then in uplink (UL) [7]. In DL, the UE must be able to perform initial synchronization to establish a successful connection with the best serving eNodeB. To accomplish this process, NR has defined two kinds of synchronization signals: NR-PSS and NR-SSS [8]. And they are based on cyclic prefix orthogonal frequency division multiplexing (CP-OFDM) [8]. However, orthogonal frequency division multiplexing Access (OFDMA) signal is highly sensitive to synchronization error, which results in inter-carrier interface (ICI). Therefore, the UE needs precise DL synchronization to protect the orthogonality between sub-carriers and wipe off ICI. In actual transmission system, the UE firstly detects the position of the NR-PSS to acquire the symbol timing and also determines the sector index. Then the UE estimates the CFO and compensates the CFO of the received signal. Finally, the UE identifies the cell identity (ID) group by the received NR-SSS. In UL, the eNodeB estimates the transmit timing and identifies the UE using the physical random access channel (PRACH) signal transmitted by the UE.

According to the DL synchronization description above, the NR-SSS can be identified only after the successful detection of the NR-PSS. Hence the overall DL synchronization performance heavily depends on the NR-PSS detection at the UE. This paper intends to present a NR DL initial synchronization scheme and compares the performance among the NR-PSS with different lengths by simulation.

The rest of the paper is organized as follows: Section 2 gives the system description, mainly including the DL frame structure and synchronization signal. In Section 3, the DL initial synchronization procedure is outlined and the simulation platform of the DL initial synchronization is presented in details. Simulation assumptions and results are shown in Section 4. Finally, Section 5 concludes this paper.

MOBIMEDIA 2017, July 13-14, Chongqing, People's Republic of China

DOI 10.4108/eai.13-7-2017.2270278

2 SYSTEM DESCRIPTION

In this section, we take a brief introduction of the DL frame structure and synchronization signal.

2.1 Frame structure

While both frequency division multiplexing (FDM) and time division multiplexing (TDM) of the synchronization signal are proposed in NR, a study focusing on TDM is undertaken in this paper. Unlike LTE, which only supports one numerology, in NR, multiple numerologies are supported because a single OFDM numerology can not achieve the performance requirements for all the deployment scenarios and the desired frequency range [9]. As a result, a family of SCS with a basic SCS scaled by integer multiples are allowed. The basic SCS can be 15kHz for forward compatibility. In this paper, we only consider low frequency case (e.g. below 6GHz) and thus two possible SCS are chosen, 15kHz and 30kHz respectively.

In NR, the frame structure design is similar with that in LTE, but the number of the symbols in a slot and the number of the slots in a sub-frame are changed with the SCS. Concretely, a sub-frame duration is fixed to 1 ms and a radio frame duration is 10ms [8]. There are two types of cyclic prefixes (CP): the normal CP and the extended CP. In the normal CP type, either 7 or 14 consecutive OFDMA symbols, depending on whether the 15kHz SCS or 30kHz SCS is used, form one slot. Figure 1 shows the frame structure with 15kHz SCS and the normal CP when the bandwidth equals 5MHz, the duration of CP is $40T_s$ for the first OFDMA symbol and $36T_s$ for the remaining 6 OFDMA symbols in each slot, where T_s is the basic time unit. Figure 2 shows the frame structure with 30kHz SCS in the same condition, the duration of CP is $22T_s$ for the first OFDMA symbol and $18T_s$ for the remaining 13 OFDMA symbols in each slot.

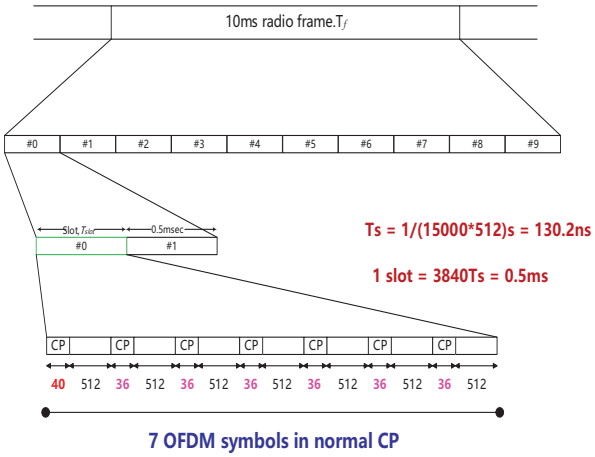

Figure 1: Frame structure with 15kHz SCS

2.2 Synchronization signal

The NR synchronization signal contains the NR-PSS and NR-SSS. In frequency domain, NR-PSS and NR-SSS are mapped on the sub-carriers of equal length located at the centered frequency band for all transmission bandwidth. In time domain, both synchronization sequences are generated as an OFDMA symbol respectively and are mapped on different symbols. For NR-PSS, Zadoff-Chu (ZC) sequence, which has constant-amplitude zero autocorrelation (CAZAC) property, can be used as the baseline sequence for study [8]. A ZC sequence of odd length L is defined as

$$d_u(k) = e^{-j\frac{\pi uk(k+1)}{L}} \qquad 0 \le k < L, \tag{1}$$

where u is the ZC root index relatively prime to L.

NR-SSS is constructed by pseudo noise (PN) sequences and carries the information related to the frame timing and the cell ID.

In reference [10], numerous proposals about NR synchronization signal design are summarized. For NR-PSS design, we can classify various proposals according to four criteria: sequence length, number of PSS sequences, central-symmetry and time repetition. We mainly concentrate on the evaluation for NR-PSS design with various lengths in this paper.

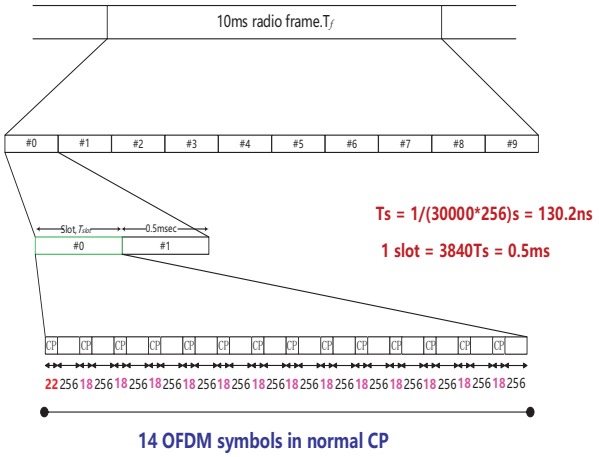

Figure 2: Frame structure with 30kHz SCS

3 DL INITIAL SYNCHRONIZATION SIMULATION PLATFORM

The DL transmitted signal propagates through a multi-path fading channel and arrives at the receiver. Under the impact of a frequency misalignment between the transmitter's and the receiver's oscillators, doppler frequency shift and the additive white Gaussian noise (AWGN), the received signal is distorted, which leads to the degradation of the synchronization system performance. To combat the problem, the DL initial synchronization procedure usually consists of three steps shown in Figure 3, firstly primary synchronization for detection of symbol timing and sector cell index, then CFO compensation with the estimated CFO, and finally secondary synchronization for detection of cell ID group and frame timing. In this paper, we developed a platform to simulate

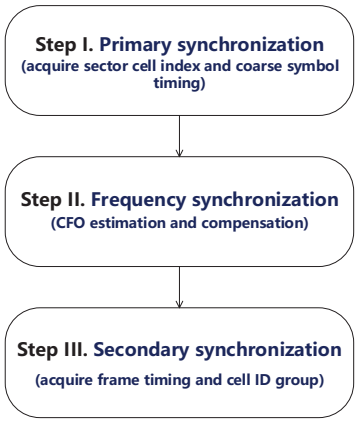

Figure 3: The DL Initial synchronization flow chart

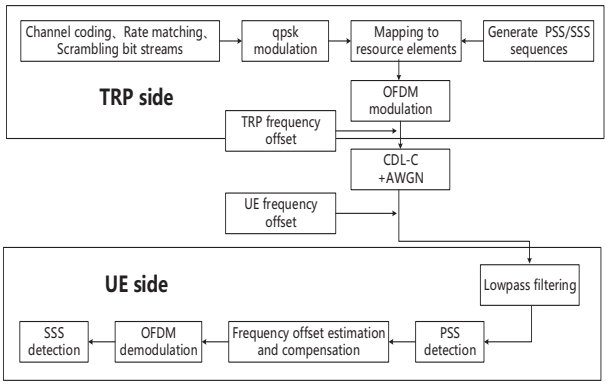

Figure 4: The DL Initial Synchronization Simulation Platform

the DL initial synchronization illustrated in Figure 4. The platform is described as follows.

3.1 Overall description of the platform

In the transmitter, two frames are transmitted. The user data is randomly generated and modulated by Quadri Phase Shift Keying (QPSK). Synchronization symbols are generated and inserted into the OFDM time-frequency grid. In the time domain, the NR-PSS is located in the the last OFDMA symbol of the first and 11th slots within the radio frame and the NR-SSS is located in the symbol preceding the NR-PSS. In the frequency domain, the NR-PSS and NR-SSS are both mapped to the centered frequency band. The modulated data symbols are then mapped to the resource elements which are not occupied by synchronization symbols. The DL signal is transmitted after the OFDM modulation.

In the receiver, the UE firstly performs a low-pass filtering. Then the NR-PSS is detected to acquire the symbol timing, sector cell index and the IFO estimation. After this, the FFO is estimated by a method called cross-correlation synchronization algorithm using PSS [11]. Finally, the NR-SSS is detected to identify the cell ID group and the frame timing.

In the following, we describe the main algorithms in our platform. The time-domain received signal is denoted by $r(\theta)$, the time-domain signal of the NR-PSS sequence by $p(\theta)$, the fast Fourier transform (FFT) size by N, the length of CP by L, the length of the NR-SSS sequence in the frequency domain by L_{SSS}, the estimation of the timing synchronization position of NR-PSS by $\hat{\theta}$, the estimation of cell sector index by $\hat{i}$, the estimation of the IFO with respect to the SCS by $\hat{\varepsilon}_I$, the estimation of the FFO with respect to the SCS by $\hat{\varepsilon}_F$, the estimation of the CFO with respect to the SCS by $\hat{\varepsilon}$, the estimation of the cell ID group by $\hat{j}$ and the estimation of the sub-frame index number by $\hat{ns}$.

3.2 Primary synchronization

The NR-PSS is transmitted periodically. A transmit period is the minimum length of the search window. In a search window, The receiver performs the NR-PSS detection by the matched filtering operation between the local NR-PSS signal and the received signal under different timing position and frequency offset hypothesis in the time domain [12]. Concretely, a timing metric function for the NR-PSS detection is defined as

$$\boldsymbol{M}(\theta, i, \varepsilon_I) = \frac{|\gamma(\theta, i, \varepsilon_I)|}{\xi_i(\theta)}, \tag{2}$$

where

$$\gamma(\theta, i, \varepsilon_I) = \sum_{n=1}^{N} r(\theta + n) e^{-j2\pi\varepsilon_I n/N} p_i^*(n), \tag{3}$$

$$\xi_i(\theta) = \frac{\sum_{n=1}^{N} \left|r(\theta + n)\right|^2 + \sum_{n=1}^{N} \left|p_i(n)\right|^2}{2}, \tag{4}$$

are the cross-correlation term and the energy term, respectively. Then the timing position of the NR-PSS, the cell sector index and the estimation of the IFO can be decided by the criterion

$$\{\hat{\theta}, \hat{i}, \hat{\varepsilon}_I\} = arg \max_{\theta, i, \varepsilon_I} \boldsymbol{M}(\theta, i, \varepsilon_I). \tag{5}$$

In addition, in the large frequency offset case, the partial correlation, where each segment is correlated separately and segment accumulations can partially make up for the phase difference and obtain lager gain, improve the performance of the NR-PSS detection[13]. However, the performance will degrade as the number of the segments increases.

In this paper, three frequency offset hypotheses (e.g. -1, 0, 1 of the SCS) and 2-segment partial correlation are adopted for the NR-PSS detection after different combinations of the number of frequency offset hypotheses and partial correlations are compared.

3.3 Frequency synchronization

For the OFDMA system, it can make efficient use of available bandwidth without distortion. However, it is susceptive to the CFO (due to a frequency misalignment between the

transmitter's and the receiver's oscillators as well as Doppler shifts), which causes the ICI by destroying the orthogonality between sub-carriers. To improve the synchronization detection performance, the CFO has to be compensated before demodulating the OFDMA symbol. The CFO is the sum of the IFO and the FFO, and the estimation of the IFO has been derived by the primary synchronization. Then the FFO can be estimated by the cross-correlation synchronization algorithm using PSS. In details, the IFO is first compensated to mitigate the impact of the IFO and the FFO is then estimated by

$$\hat{\varepsilon}_F = \frac{1}{\pi}\angle([\sum_{n=0}^{N/2-1} r(\hat{\theta}+n)e^{-j2\pi\hat{\varepsilon}_I n/N}p_i^*(n)]^* \cdot [\sum_{n=N/2}^{N-1} r(\hat{\theta}+n)e^{-j2\pi\hat{\varepsilon}_I n/N}p_i^*(n)]). \quad (6)$$

Finally we acquire the CFO by $\hat{\varepsilon} = \hat{\varepsilon}_I + \hat{\varepsilon}_F$. and fulfill the frequency synchronization by compensating the CFO using $z(n) = r(n)e^{-j2\pi\hat{\varepsilon}n/N}$.

3.4 Secondary synchronization

The NR-SSS carries the information including the radio frame timing and the cell ID group. It is formed based on two groups of proposals [14]: long PN sequences (like m-sequences, Gold sequences, ZC) and interleaving two short m-sequences (like LTE-SSS). The basic sequences are scrambled with the cell sector index and the cell ID group related parameters. The NR-SSS detection is done based on the relative position between the NR-PSS and the NR-SSS. According the timing synchronization position of the NR-PSS, the timing synchronization position of the NR-SSS can be figured out and then the time-domain signal of the NR-SSS is extracted. After FFT and rearranging the location of the sub-carriers in NR-SSS, we obtain the NR-SSS sequence in the frequency domain. In the end, we perform a cross-correlation operation between the demodulated NR-SSS sequence, denoted by r_{sss}, and the known local NR-SSS sequences, denoted by $s_{j,ns}(n)$. In details, the operation is defined as

$$\boldsymbol{C}(j,ns) = \left|\sum_{n=1}^{L_{sss}} r_{sss}^*(n)s_{j,ns}(n)\right|. \quad (7)$$

When the metric $\boldsymbol{C}(j,ns)$ achieves the peak value, the cell ID group and the sub-frame index number can be estimated, namely

$$\{\hat{j},\hat{ns}\} = arg\max_{j,ns}\boldsymbol{C}(j,ns). \quad (8)$$

4 SIMULATION ASSUMPTIONS AND RESULTS

In this paper, we mainly focus on the low frequency (below 6GHz) case with 4GHz carrier frequency. To fairly evaluate the performance of the proposed NR-PSS sequences with different lengths, we assume the same bandwidth and a fixed OFDMA symbol transmission power for all schemes. Thus the FFT size is set at 512/256 for SCS of 15/30kHz accordingly. In addition, we further assume the timing is correct when the residual timing offset is within half CP length and the frequency offset estimation is sound when the residual frequency offset is within 1 SCS. For the multi-path fading channel environments, the Clustered Delay Line (CDL-C) model [15] which is recommended by 3GPP is considered. For the AWGN channel environments, the signal-to-noise ratio (SNR) is set at -6dB. The simulation parameters are listed in Table 1.

Table 1: SIMULATION PARAMETERS

Parameter	Value
Sampling frequency	7.68MHz
Carrier frequency	4GHz
System bandwidth	5MHz
SCS	15kHz/30kHz
FFT size	512/256
Cyclic prefix type	Normal CP
Search window	5ms
Multiplexing	TDM
SNR	-6dB
Channel model	CDL-C with delay scaling values of 100ns +AWGN
UE speed	3km/h
Antenna configuration at the TRP	(1,1,2) with omni-directional antenna element
Antenna configuration at the UE	(1,1,2) with omni-directional antenna element
Frequency Offset	TRP: uniform distribution +/-0.05 ppm UE: uniform distribution +/-5 ppm
Number of interfering TRPs	0

In the simulation, we only concentrate on the first and second DL initial synchronization step because we only evaluate the performance of the NR-PSS sequences with different lengths by residual timing offset and residual frequency offset. Three cases where the lengths of the NR-PSS sequences are set to 63, 127, 255, respectively and the corresponding root indexes are set to 25, 42, 116, respectively are simulated, thus we acquire two figures, which present the cumulative distribution function of the residual timing offset and the cumulative distribution function of the residual frequency offset, respectively.

In Figure 5, the cumulative distribution function of the residual timing offset at different case $L = 63, L = 127, L = 255$ is shown. From Figure 5, we can observe that the performance becomes better as the increase of L under the same SCS due to higher time resolution. In Figure 6, the cumulative distribution function of the residual frequency offset at different case $L = 63, L = 127, L = 255$ is presented. From Figure 6, we can see the sequences with different lengths

perform equally well under the same SCS. Hence, we conclude the longer sequences are better choices for the NR-PSS design from improving the performance of the residual timing offset and residual frequency offset.

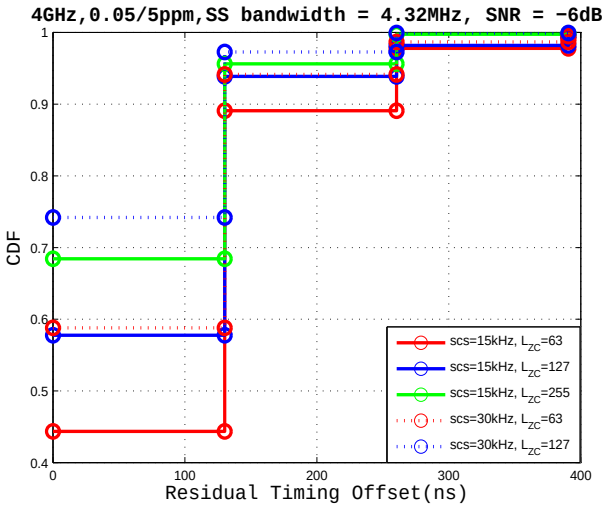

Figure 5: Comparison of Residual Timing Offset

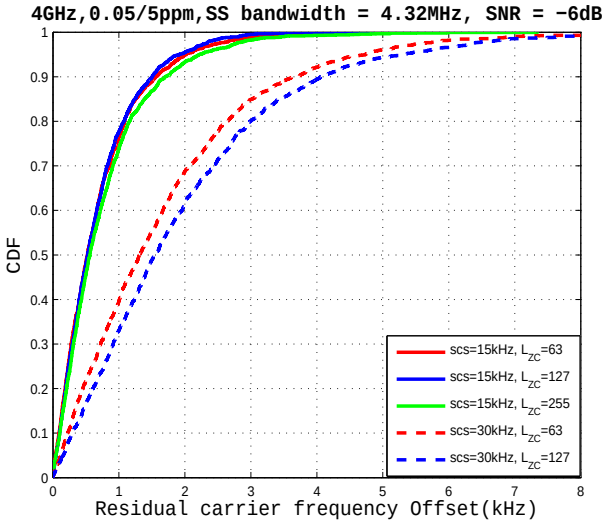

Figure 6: Comparison of Residual frequency Offset

5 CONCLUSIONS

In this paper, the different frame structures under different SCS (15kHz, 30kHz) are first introduced. Then we describe the DL initial synchronization procedure in a nutshell, and the platform we designed to perform the DL initial synchronization is presented in details. Finally we simulate the different NR-PSS design with different lengths. It is observed that longer sequences has better performance in residual timing offset and the length of the sequences does not have an impact on the performance in residual frequency offset under the same SCS. We conclude the paper by proposing the longer sequences in NR-PSS design if the performance of residual timing offset and residual frequency offset is only considered.

6 ACKNOWLEDGEMENT

This work was supported by the National Natural Science Foundation of China (Grant No. 61501045) and the State Major Science and Technology Special Projects (Grant No. 2016ZX03001017-004).

REFERENCES

[1] M. Agiwal, A. Roy, and N. Saxena, "Next generation 5G wireless networks: a comprehensive survey," *IEEE Commun. Surveys Tuts.*, vol. 18, no. 3, third quarter 2016, pp. 1617-1655.

[2] "5G radio access-research and vision," Ericsson White Paper, Jun. 2013. [Online]. Available: http://www.ericsson.com/news/130625-5g-radio-access-research-and-vision_244129228_c

[3] "5G: New air interface and radio access virtualization," Huawei White Paper, Apr. 2015. [Online]. Available: http://10.3.200.202/cache/3/03/huawei.com/a7d44f9c163d9a8836d1fc09f438db30/5g_radio_whitepaper.pdf

[4] Z. Zhao, M. Peng, Z. Ding, C. Wang, and H. V. Poor, "Cluster formation in cloud-radio access networks: Performance analysis and algorithms design," in *Proc. IEEE ICC*, London, UK, Jun. 2015, pp. 3903 - 3908.

[5] Z. Zhao, M. Peng, Z. Ding, W. Wang, and H. V. Poor, "Cluster content caching: an energy-efficient approach to improve quality of service in cloud radio access networks," *IEEE J. Sel. Areas Commun.*, vol. 34, no. 5, May 2016, pp. 1207-1221.

[6] Z. Zhao, Y. Ban, D. Chen, Z. Mao, and Y. Li, "Joint design of iterative training-based channel estimation and cluster formation in cloud-radio access networks," *IEEE Access*, vol. 4, Oct. 2016, pp. 9643-9658.

[7] W. Xu, and K. Manolakis, "Robust synchronization for 3gpp lte system," in *Proc. GLOBECOM*, Miami, Florida, USA, Dec. 2010, pp. 1-5.

[8] 3GPP TR 38.802 version 1.2.0:"Study on New Radio (NR) Access Technology, Physical Layer Aspects," Feb. 2017.

[9] J. Vohriälä, A. A. Zaidi, V. Venkatasubramanian, N. He, E. Tiirola, J. Medbo, E. Lähetkangas, K. Werner, K. Pajukoski, A. Cedergren, and R. Baldemair, "Numerology and frame structure for 5g radio access," in *Proc. PIMRC*, Valencia, Spain, Dec. 2016, pp. 1-5.

[10] R1-1704860, "Summary of 88-12 email discussion on NR-SS design," LG Electronics, 3GPP TSG RAN WG1 Meeting #88bits, Spokane, USA, Apr. 2017.

[11] S. Huang, Y. Su, Y. He, and S. Tang, "Joint time and frequency offset estimation in LTE downlink," in *Proc. ICST*, Kunming, China, Aug. 2012, pp. 394-398.

[12] R1-1700037, "Synchronization signals for NR," Huawei, HiSilicon, 3GPP TSG RAN WG1 NR Ad Hoc Meeting, Spokane, USA, Jan. 2017.

[13] Y. Yu, and Q. Zhu, "A novel time and frequency synchronization for 3GPP LTE cell search," in *Proc. ICST*, Guilin, China, Aug. 2013, pp. 328-331.

[14] R1-1705564, "Synchronization signal bandwidth and sequence design," Qualcomm Incorporated, 3GPP TSG-RAN WG1 #88bis, Spokane, USA, Apr. 2017.

[15] 3GPP TR 38.900 version 14.1.0:"Study on channel model for frequency spectrum above 6 GHz," Sep. 2016.